Proceedings of the ASME 2011 International Design Engineering Technical Conferences & Computers and Information in Engineering Conference
IDETC/CIE 2011
August 29-31, 2011, Washington, DC, USA

DETC2011-48513

OPTIMAL COMPONENT SIZING AND FORWARD-LOOKING DISPATCH OF AN ELECTRICAL MICROGRID FOR ENERGY STORAGE PLANNING

John W. Whitefoot*
Optimal Design Laboratory
University of Michigan
Ann Arbor, Michigan USA

Abigail R. Mechtenberg
Optimal Design Laboratory
University of Michigan
Ann Arbor, Michigan USA

Diane L. Peters
Optimal Design Laboratory
University of Michigan
Ann Arbor, Michigan USA

Panos Y. Papalambros
Optimal Design Laboratory
University of Michigan
Ann Arbor, Michigan USA

ABSTRACT

Optimal design of an electrical microgrid and sizing of its components seeks to balance capital investment with expected operational cost while meeting performance requirements. Calculating operational cost requires scheduling each microgrid component over some time period (dispatching) for each design evaluated. Heuristic or rule-based dispatch strategies typically consider only single time instances and are computationally efficient but do not include scheduling energy storage for future time periods. In this paper, we propose to optimize microgrid designs using forward-looking optimal dispatch for future energy storage planning. We present a case study of an 'islanded' military base microgrid with renewable and non-renewable electricity generation, battery storage, and plug-in vehicles with electrical export power capability. The optimal design and forward-looking dispatch strategy are compared to results obtained using the publicly available rule-based dispatch strategy in HOMER Energy software. Results show that the forward-looking strategy uses storage batteries to plan for future energy shortfalls rather than simply as a buffer for variable renewable energy supply, resulting in a 7.8% reduction in predicted fuel use. For the given cost assumptions, sensitivity analysis of the optimal design with respect to fuel price shows that investment in renewable energy technology is justified at prices greater than $5 per gallon ($1.32/liter) with an attendant reduction in fuel use of 3–30%.

1 INTRODUCTION

Installing on-site energy generation offers the potential to reduce energy use and greenhouse gas emissions while increasing local energy security. These energy generation and storage devices, collectively called distributed energy resources (DERs), can be networked into a local electrical system called a microgrid. These microgrids have the ability to operate connected to or independent from the external electrical grid, and are particularly useful when energy security is important, and/or where electrical distribution infrastructure does not exist. Example applications include military bases [1], medical complexes, island communities [2], and remote towns [3,4].

Designing a microgrid is often done using the expected peak load on the system, but this is a conservative approach that has the potential to oversize components, especially if the dispatch (operation and scheduling) of the components is not considered simultaneously to the system design. This necessitates a coordinated, system-level design and dispatch problem that considers the sizing of individual DER elements and their dispatch control strategy.

The complexity of solving the microgrid design problem is due to having to evaluate each design by determining the operation of the microgrid at discrete time steps over some time period. Much previous work developed various approaches for solving this dispatch problem, including linearization and solving a multi-period linear program [4–7], nonlinear programming over fixed time periods [8], use of derivative-free methods to solve individual time increments for minimum cost [9], sequential solution of each individual time period using a rule-based dispatch strategy [10], and decomposition of the time period into increments that are coordinated and solved using multi-disciplinary optimization (MDO) techniques [11]. These dispatch solution approaches typically use historical data for power loads, renewable energy supply, etc. and assume perfect knowledge (no uncertainty) to solve for the dispatch strategy. Other research has used model-predictive control to better represent actual microgrid operation to solve the multi-period dispatch problem with a finite time horizon using expectations of system inputs and future microgrid states [12].

A subset of this research also considers the optimal design of the microgrid in addition to solving the dispatch problem. Stadler et al. pose the design and dispatch problem as a an All-in-One (AiO) problem for the entire year by linearization and solution using linear programming [7], thus increasing solution efficiency but at the limitation of linearizing submodels, such as diesel generator efficiency as a function of load, battery internal resistance as a function of state-of-charge, etc. Lu et al. solve a nonlinear microgrid design problem by decomposing it using

* Corresponding author, johnjohn@umich.edu

MDO techniques to solve each time increment individually while coupled to other time increments through battery storage linking variables [11]. However, their approach does not calculate a multi-component optimal dispatch; instead, they use non-dispatchable components (wind and solar) to determine when battery storage should charge or discharge. In addition, they solve the problem using one-day time increments, which does not consider the hourly dynamics of renewable energy supply and energy storage. Asano and Bando solve a nonlinear design and dispatch problem by separating the year into six representative days, then solving each day as a fixed AiO problem [8]. However, their approach does not consider the boundaries of the solved days by linking the time before and after the representative days. As such, the approach provides an approximation of the microgrid performance, but may differ from how the microgrid will be controlled and operated in practice. HOMER Energy solves the optimal design problem using a full-factorial design of experiments on number and size of components, and uses a rule-based dispatch strategy to evaluate the microgrid operation. Their approach solves the dispatch strategy for minimum cost in a single time increment without explicitly planning energy storage for future time increments [10].

Of the microgrid optimal design and dispatch approaches, only Momber et al. consider the dynamics of plug-in electric vehicles (PEVs), which have the added complexity of time-dependent connection or disconnection to the microgrid [13]. Though HOMER Energy software can model scheduled generators, it does not currently have the ability to model scheduled energy storage (such as a PEV), nor coupled components, such as a vehicle engine charging a battery pack.

This paper proposes a new approach to solve the combined optimal design and dispatch strategy for a microgrid using nonlinear component submodels and solving the optimal dispatch using a moving time horizon to link the microgrid operation before and after each window of time. In addition, the problem formulation can consider time-variant connection of components to model the interaction of PEVs. This approach will take advantage of forward-looking energy storage scheduling while also approximating realistic control methods, such as model-predictive control (MPC). A case study is presented to solve the optimal design and electrical dispatch of an islanded military base supplied by diesel generators, battery storage, photovoltaic solar panels, and plug-in vehicles. The results will be compared to the design and dispatch of a similar system using HOMER Energy software as a benchmark.

2 METHODOLOGY

The modeling of the microgrid and the methods used for performing optimal design with forward-looking optimal dispatch are as follows.

2.1 Microgrid Model

A hub-based microgrid model similar to [14] was implemented in Matlab. In this model, a microgrid is separated into a network of power conversion and storage hubs, where each hub can contain various energy storage and conversion devices. An example microgrid hub is shown in Fig. 1.

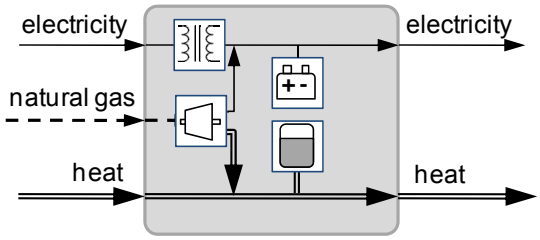

Figure 1. Example microgrid hub with energy conversion and storage devices

Each hub can be mathematically represented by Eq. 1:

$$\boldsymbol{L} = \boldsymbol{CP} - \boldsymbol{S\dot{E}} \tag{1}$$

where $\boldsymbol{L}$ is a vector of power loads required at each hub (electricity, heat, etc.), $\boldsymbol{P}$ is a vector of power inputs to the hub (electricity, natural gas, steam heat, etc.), $\boldsymbol{C}$ is a matrix of power conversion factors to determine how each power input is transmitted or converted into a power output, $\dot{\boldsymbol{E}}$ is a vector of changes in stored energy, and $\boldsymbol{S}$ is a matrix of conversion efficiencies of the energy storage devices. This system of equations is solved for each time increment, t. The conversion factors c and s are constant for a single time increment, though they may change nonlinearly with system state. For more details on hub-based microgrid modeling, refer to [14, 15].

The individual hub models are connected in a network that uses conservation of energy to calculate power transmission and transmission losses. In this implementation, transmission losses are modeled as a constant transfer efficiency, η_{TR}, of the power transferred between hubs. This implementation only calculates bulk power flows and does not consider reactive power or electrical dynamics within the system.

To satisfy conservation of energy, one dispatchable element of the microgrid is treated as 'dependent', and its dispatch is determined by the power production and consumption of the rest of the system. In a grid-connected system this can be represented by the external grid, but for an islanded system (not grid-connected) one device must be selected as the dependent element. This is shown in Eq. 2, where a diesel generator is operated as the dependent device and its dispatch is determined by the power balance of the system.

$$P^t{}_{gen} = \max(0, \sum_i P_i^t) \tag{2}$$

In this equation, P_i is the power input to hub i and P_{gen} is the generator output, solved at time t. If the net power required by the hubs is negative, i.e. if they are producing more power than they require, the dependent generator is run at zero load and the excess energy is assumed to be fed to ground or otherwise dissipated.

2.2 Optimization Problem Formulation

The overall objective of the microgrid design problem is to minimize the cost of implementing and operating a microgrid for some given area. For an islanded microgrid running mainly on diesel generators, the objective becomes minimizing the

combined annual fuel costs and annualized capital costs. Variables for the optimization include the size of DER components, number of vehicles, and dispatch of the DER components at each time step. The operating cost of the system is determined by solving the optimal dispatch problem, and the optimal dispatch is typically different for each microgrid design; thus, the optimal dispatch problem is nested within the optimal design problem. The design and dispatch problems cannot be solved simultaneously (all-in-one) because, to make the problem tractable, the optimal dispatch problem is setup as a series of optimization problems solved over a moving time window. If the optimal dispatch problem was known to be convex, this nested problem structure could be proven to provide the global optimal design [16]. However, in the current formulation there are non-convex functions within the dispatch problem, thus there is the possibility for multiple optima and no generalities can be made about global optimality or combined optimality.

A generalized problem structure is shown in Figure 2. The optimal design problem (outer loop) passes a vector of design variables to the optimal dispatch problem (inner loop). These design variables are treated as parameters (held fixed) by the optimal dispatch problem. The optimal dispatch problem is solved over a 24-hour time horizon (t_0 to t_{horiz}) and then stepped forward one hour in time and re-solved, until the entire time period of interest (T_1 to T_{final}) is completed. For each time horizon, only the vector of optimal dispatch for the first time step, t_0, is saved as part of the overall optimal dispatch matrix, $\hat{\boldsymbol{u}}(\boldsymbol{T},\boldsymbol{x})$. At the end of the series of optimal dispatch problems (inner loop), the optimal dispatch matrix is returned to the optimal design problem along with the total fuel use over the time period from T_1 to T_{final}, $f_2(\boldsymbol{x},\hat{\boldsymbol{u}})$, and the feasibility information of the optimal dispatch problem, $\hat{\boldsymbol{g}}$ and $\hat{\boldsymbol{h}}$.

Optimizing the dispatch over a forward-looking time horizon is necessary to determine the optimal energy storage strategy, which requires decision-making over multiple time increments. Ideally the entire time period from T_1 to T_{final} would be solved simultaneously, but it is necessary to decompose the time period into a series of overlapping time windows (the time horizon) because solving the optimal dispatch for all time increments simultaneously is computationally infeasible, especially for a nonlinear problem. The dimension of the dispatch optimization problem increases linearly with the number of hours solved simultaneously; for example, solving the optimal hourly dispatch for a single DER over an entire year requires 8760 variables, which quickly becomes intractable for nonlinear programming algorithms. In this case, a 24-hour time horizon was chosen because the solar supply and power loads also follow a 24-hour cycle. Some optimal dispatch approaches only optimize for individual hours sequentially to reduce their computational requirements but these approaches cannot take advantage of look-ahead planning of the energy storage.

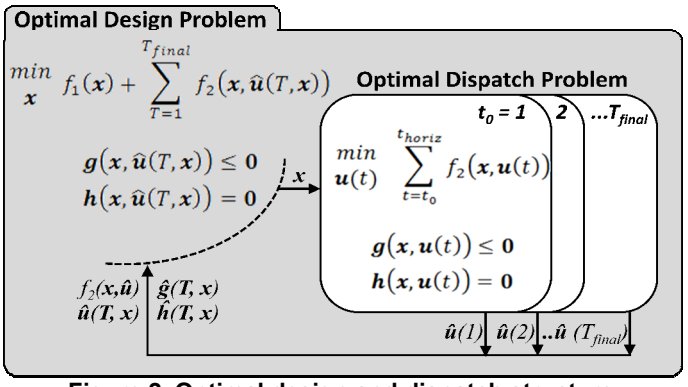

Figure 2. Optimal design and dispatch structure

As mentioned in the Introduction section, many approaches for solving optimal dispatch use linearized submodels and linear or quadratic programming, but this model uses nonlinear submodels for the generator efficiency, and energy storage efficiency is discontinuous based on whether it is charging or discharging. Therefore, a nonlinear programming algorithm, sequential quadratic programming (SQP), was used to solve the optimal dispatch problem. The SQP code chosen was the *fmincon* function in Matlab using an active-set strategy and finite-differencing to calculate gradients. It could be possible to linearize the model and solve it more quickly using linear programming, but this would result in an unknown reduction in fidelity, especially considering the nonlinear efficiency of diesel generators when operating at low load. The optimal dispatch formulation for a single time horizon is shown below.

Min: $\sum_{t=1}^{t_{horiz}} p_{fuel} E_{fuel}^t$ fuel cost for time horizon

w.r.t.:

ν_{gen2}^t	% load of secondary generator, $\forall t$
ΔSOC_{stat}^t	change in stationary battery SOC, $\forall t$
$\Delta SOC_{veh_k}^t$	change in vehicle battery SOC, $\forall t, \forall k$

subject to:

$\underline{E}_{stat} \le E_{stat}^t \le \overline{E}_{stat}$	stationary batt. energy limits, $\forall t$
$\underline{E}_{veh} \le E_{veh_k}^t \le \overline{E}_{veh}$	vehicle batt. energy limits, $\forall t, \forall k$
$\sum_i P_i^t \le \bar{P}_{gen1}^t$	main generator min. power, $\forall t$
$\Delta SOC_{veh_k}^t con_k^t = 0$	vehicle connectivity, $\forall t, \forall k$

$0 \le \nu_{gen2}^t \le 1.0$	$\forall t$
$-10\% \le \Delta SOC_{stat}^t \le 10\%$	$\forall t$
$-30\% \le \Delta SOC_{veh_k}^t \le 30\%$	$\forall t, \forall k$

$$t \in \{1,..,24\};\ k \in \{1,..,N_{vehicles}\};\ con \in \{0,1\}$$

In the preceding formulation, t is the current time increment, k is the vehicle index, con_k^t is the vehicle connectivity parameter of vehicle k at time t (where connected = 0), i is the hub index, p_{fuel} is the fuel price, E_{fuel} is the fuel energy used, E_{stat} is the stationary battery energy, E_{veh} is the vehicle battery energy, P_i is

the power input required at hub i, P_{gen1} is the main generator power, and overbars and underbars represent upper and lower limits, respectively. The addition of the vehicle connectivity equality constraint allows for the vehicle connectivity vector (binary) to define when a vehicle is attached to the microgrid, and therefore when charging or discharging can be non-zero.

Solving the series of SQP problems for the optimal dispatch results in a numerically noisy function for operating cost because small changes in algorithm convergence propagate through the series of SQP problems. Therefore, the optimal design problem was solved using the DIRECT derivative-free algorithm, which can handle noisy objective functions [17]. The design optimization formulation is presented below.

Min: annualized capital cost + annual fuel cost

$$\sum_x \frac{1}{L_x} p_x x + \sum_{T=1}^{T_{final}} p_{fuel} E_{fuel}^T$$

w.r.t.:

N_{veh}	number of plug-in vehicles (integer)
$\bar{E}_{veh}$	vehicle battery energy capacity (kWh)
$\bar{E}_{stat}$	stationary battery energy capacity (kWh)
$\bar{P}_{PV}$	photovoltaic panel peak power (kW)
$\bar{P}_{gen1}$	main generator max. power (kW)
$\bar{P}_{gen2}$	secondary generator max. power (kW)

subject to:

$\bar{P}_{gen2} \geq P_{crit}$ critical power maintenance

$\hat{\boldsymbol{g}}(\hat{\boldsymbol{u}}) \leq \mathbf{0}$, $\hat{\boldsymbol{h}}(\hat{\boldsymbol{u}}) = \mathbf{0}$ } optimal dispatch problem feasibility

$1 \leq N_{veh} \leq 5$
$3 \leq \bar{E}_{veh} \leq 20$ kWh
$20 \leq \bar{E}_{stat} \leq 80$ kWh
$20 \leq P_{PV} \leq 160$ kW
$10 \leq \bar{P}_{gen1} \leq 120$ kW
$10 \leq \bar{P}_{gen2} \leq 120$ kW

In the preceding formulation, p_x is the capital cost for component x, L_x is the expected lifetime of component x, $P_{critical}$ is the maximum power required at the critical hub, $\hat{\boldsymbol{g}}$ and $\hat{\boldsymbol{h}}$ are vectors containing the values of the dispatch problem inequality and equality constraints at its optimum ($\hat{\boldsymbol{u}}$), and the other variables are defined in the problem statement.

The objective is a function of both the annualized capital costs (design) and the annual operating costs from the optimal dispatch problem. Most of the constraints on the design problem are simple bounds on the size of the components. The critical power constraint ensures that the critical hub can be maintained by the secondary generator alone, in the event that part of the microgrid fails (explained in detail in the Case Study section). Lastly, there is a constraint to ensure feasibility of the optimal dispatch problem.

3 CASE STUDY

As a case study to implement this approach, a small military forward-operating base (FOB) was modeled. These bases typically operate islanded (not connected to an external electrical grid) and the electrical power is provided by diesel generators, which often operate at low-efficiency, part-load conditions due to the changing electrical demand. The fully-burdened cost of fuel for the U.S. Army can range upwards from $5 per gallon ($1.32/liter), with one study estimating the full cost of a gallon of JP-8 at $13.68/gallon ($3.61/liter) [18]. Thus, the capital investment in renewable energy could be justified to reduce fuel cost.

In addition, the military is investigating the use of plug-in vehicles to support these FOB microgrids. Future military vehicles, such as the proposed Joint Light Tactical Vehicle (JLTV), will have significant on-board electrical power generation, potentially offering up to 30 kW of export power as well as modest battery storage. During vehicle operation this will be used for auxiliary electrical loads rather than vehicle propulsion, but when the vehicles are parked they could provide additional storage for the microgrid as well as power generation capability.

The hypothetical forward-operating base (FOB) modeled for this study is a small, 50-soldier FOB near Kabul, Afghanistan. The base is remote and thus its microgrid is islanded from any external grid. The microgrid is modeled as four separate hubs, radially connected from a central power-supply hub as shown in Figure 3. The main power hub (Hub 1) contains the main diesel generator, photovoltaic array, and lead-acid stationary battery. The other hubs consist of a vehicle connection hub (Hub 2), where vehicles can store or supply energy to the microgrid; a housing hub that is solely an energy consumer (Hub 3); and a "critical" hub (Hub 4) containing communications, medical treatment, etc. where power must be maintained at all times, thus it has an additional (secondary) diesel generator. In this model, the generator in Hub 1 is used as the dependent device, so its dispatch level is determined by the power balance of the rest of the system.

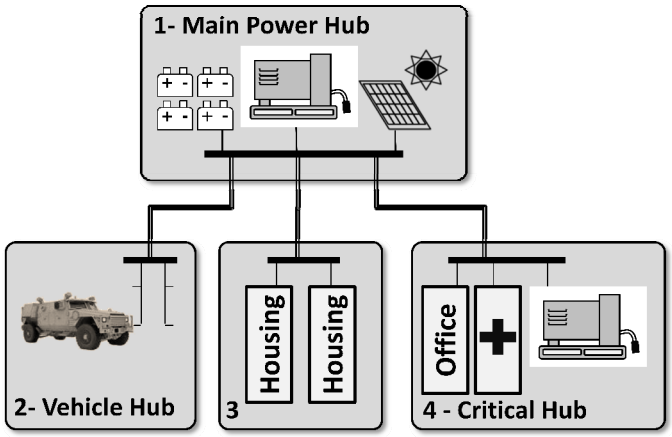

Figure 3. Schematic of microgrid hubs for the Forward Operating Base case study

3.1 Benchmarking Case

The forward-looking optimal dispatch strategy was benchmarked against the dispatch strategy in HOMER Energy's microgrid modeling software. HOMER was chosen because it is publicly available for microgrid modeling, it is quick to implement, and it has the capability of using nonlinear

submodels (e.g., for the diesel generators). As mentioned in the Introduction section, HOMER uses a rule-based strategy to sequentially decide the dispatch at each time increment, linked only to other time increments through the boundary conditions of energy storage state-of-charge (SOC). For this study, the "cycle charging" strategy was chosen within HOMER. Using this strategy, HOMER decides the minimum cost dispatch strategy at each time increment while attempting to only run diesel generators at maximum load, using excess generator power to charge energy storage. In addition, this strategy seeks to reduce battery degradation by using a soft target for the lower bound of battery SOC. For more details on HOMER's dispatch strategy, please refer to [10].

The case study was simplified in order to precisely match our model to a model in HOMER. Most importantly, HOMER does not have the capability to model coupled systems, such as a plug-in vehicle where the vehicle engine can charge the battery when it drops below a state-of-charge set point, nor is HOMER able to model batteries that are selectively connected and disconnected from the system, as is the case with a PEV. Thus, PEVs were not used for the dispatch strategy benchmarking study. Also, HOMER uses a different PV panel submodel, so its solar panel output power was directly input to our forward-looking model. The solar panel output over the entire year is shown as a density map (hour vs. day) in Fig. 4.

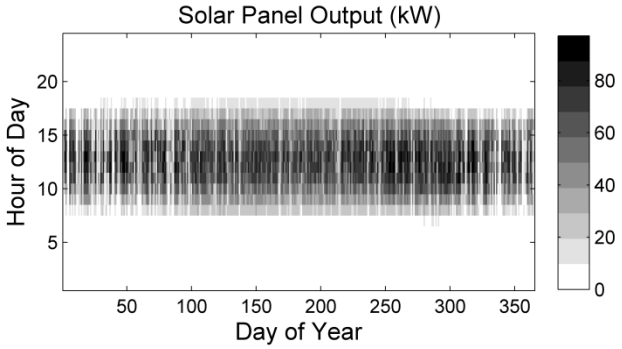

Figure 4. HOMER solar panel power output for one year near Kabul, Afghanistan

Power transmission between hubs was modeled without losses, but conversions from AC to DC, and vice versa, had efficiencies of 0.9 for each direction. Likewise, battery charging and discharging had a constant efficiency of 0.9 for each direction. The layout of the HOMER model is shown in Fig. 5.

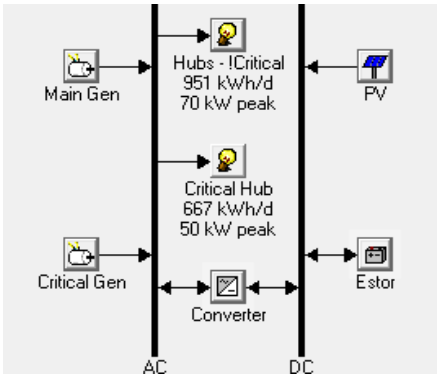

Figure 5. HOMER microgrid model used for benchmark

The other submodels that were commonized between the two models were the diesel generator efficiency and power load over the year. For the diesel generator model, generator efficiencies at various loads were gathered on Cummins diesel generators in rated powers from 10 – 300 kW [19]. A response surface model was created to calculate the generator efficiency as a function of generator size and load, with the response shown in Figure 6.

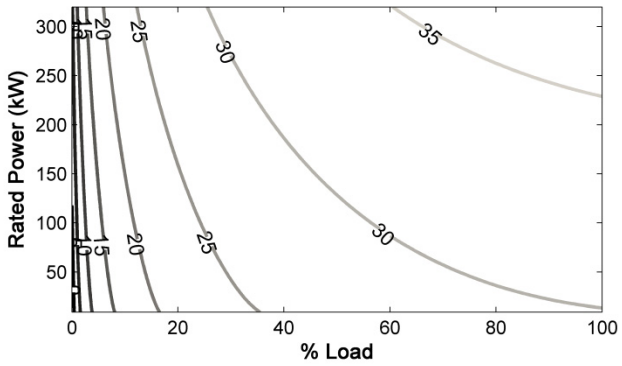

Figure 6. Model of diesel generator efficiency as a function of generator rated power and load

The electrical power load was based upon the number of soldiers at a small forward operating base (50) and the estimated average and peak power loads per soldier (1.5 – 2 kW per soldier). Due to lack of measured data, the daily power load is generically represented by a base load with an afternoon peak and night-time trough. Example power loads for each hub over one day are shown in Fig. 7.

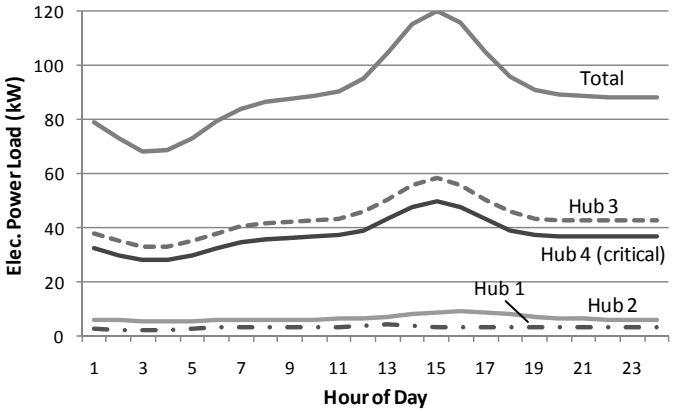

Figure 7. Power load for each hub for Jan. 15th overlaid with total load

These base power loads for a given day were modified by seasonal average temperature data for the chosen region by Eq. 3, where the deviation from a "goal" temperature is used to approximate heating and cooling load changes.

$$L_d = L_b[0.65 + 0.023max(0, T_{av} - T_g) + 0.016max(0, T_g - T_{gav})] \quad (3)$$

In this equation, L_d is the daily power load, L_b is the average power load over the year, T_{av} is the average air temperature for a given day (°F), and T_g is the goal temperature, chosen to be

65 °F. The average daily temperature for the region was taken from historical data, as shown in Table 1.

Table 1. Average monthly high and low temperature for Kabul, Afghanistan (°F) [20]

	1	2	3	4	5	6	7	8	9	10	11	12
High	40	41	54	66	75	86	89	89	83	72	59	46
Low	19	21	33	42	47	54	59	57	48	39	29	23

Nominal sizes were chosen for the microgrid components based on a HOMER sizing study with a three-level, four-variable, full-factorial design of experiments. The component sizes for the dispatch benchmarking comparison are shown in Table 2.

Table 2. Component sizes used for benchmark study

Main Generator (kW)	Critical Generator (kW)	PV panel (kW)	Storage Battery (kWh)
70	50	97	48

3.2 Design Optimization Case

To run the design optimization with forward-looking optimal dispatch, some changes were made from the dispatch benchmarking case study. The changes included addition of plug-in vehicles to the microgrid, addition of power transmission losses between hubs, a different photovoltaic model, and running the dispatch for less than a full year to increase the speed of calculating the optimal dispatch for each design. Additionally, the capital cost of the components was calculated for each design in addition to the operating costs.

The vehicles are modeled as power-export devices, where the battery pack state-of-charge can range from 30 – 100%. If the SOC drops below 30%, the vehicle engine can run an electrical generator to recharge the battery to 40% SOC. The vehicles use their diesel engines through 30 kW integrated starter/generators to provide electrical power, so the charging load is fairly low with an efficiency of 23%.

The vehicles are modeled with a fixed schedule of connection and disconnection from the grid to represent their daily use, and this schedule was randomly assigned to each vehicle based upon a 70% probability of being connected during any one-hour period. Though the schedule was randomly defined, the same schedule was used for each case studied to allow for comparison. The vehicle fuel use while driving was assumed constant and excluded from this analysis.

The efficiencies of charging both the Li-ion and lead-acid batteries, PV array inverter efficiency, and electrical line losses between hubs were modeled linearly with constant efficiencies as listed in Table 3. The batteries were modeled as perfect storage devices with losses incurred only during charging and discharging. The power output from the PV array scaled linearly with solar irradiation and rated power, which was based on a 1 kW/m^2 peak solar irradiance with a 0.95 derating factor.

Table 3. Electrical transmission and conversion efficiencies

	Transmission between hubs	Battery Charge/Discharge	PV panel Inverter
Efficiency	95%	90%	94%

The solar irradiance for the week modeled is taken from HOMER, which uses NASA satellite data at approximately this location. Due to the high variability of solar supply (due to clouds, etc.), the hourly solar irradiance was averaged using one week before and after the days studied to smooth out the supply and represent an average day at that time of year. The averaged solar irradiance used is shown in Fig. 8.

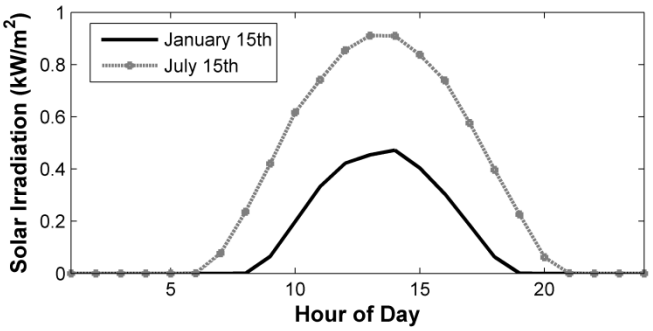

Figure 8. Averaged solar irradiance for Kabul, Afghanistan

Solving the optimal dispatch for a single design over an entire year is computationally intensive, taking 2–3 hours on a 2.8GHz, quad-core i7 processor PC with 8GB of RAM. Therefore, steps were taken to estimate the operating costs based on the optimal dispatch for representative days of the year. This approach is a modified version of Asano and Bando's [8] but in this case the representative days were linked to preceding and following days, and the total annual operating cost was estimated using these representative days.

The optimal dispatch problem was initially solved for three consecutive days during the middle of each month of the year for four different microgrid designs. Based on these results it was determined that the fuel use for one day in February, March, November and December could be related to the fuel use in January and all other months could be related to the fuel use in July using on the ratios in Table 4. Other microgrid designs were tested with this method and the prediction accuracy for each was greater than 94%. Using this approach allowed for the entire year's fuel use to be estimated by solving the optimal dispatch for three consecutive days in January and July, which substantially reduced computation time. The final optimal designs were then re-run for the entire year to get their true fuel use for comparison. It is important to note that these ratios will be different for any location studied due to differences in seasonal temperatures, solar energy supply, and base power loads.

Table 4. Ratios for estimating monthly fuel use based on January or July fuel use

Feb	Mar	Apr	May	Jun	Aug	Sep	Oct	Nov	Dec
0.95	0.75	0.99	0.81	0.88	0.98	0.82	1.05	0.80	0.95

The capital costs of the microgrid components are functions of their sizes and the capital costs were "annualized" to enable trading off with annual operating cost. The capital cost of diesel generators and photovoltaic arrays are functions of their maximum power, p (kW), and battery costs are a function of their capacity, c (kWh), as shown in Table 5.

Table 5. Capital cost equations as a function of component size

Component	Capital Cost Equation ($)	Reference
Generators	$1352(p^{0.631})$	[21]
PV array	$8431(p^{0.983}) + 3000$	[21]
Lead-acid Batt	$190c$	[22]
Li-ion Batt	$700c$	[23]

The annualized capital costs are calculated by dividing the capital cost by expected usable life (the net present value of the capital was not considered). The lifetimes were estimated based upon lifetimes reported by Lawrence Berkeley National Labs [21], but the PV life was reduced from 20 to 15 years based on the rigors of military use and portability. These lifetimes are summarized in Table 6. Of course, there is always danger in estimating capital costs due to the large uncertainty for the cost and life of a specific device as well as the unknown cost of transporting this capital equipment to remote areas. However, to perform design optimization it is necessary to estimate these capital costs in order to tradeoff with the potential energy cost savings they offer.

Table 6. Lifetime estimates for capital equipment

	Diesel Gen.	PV Array	Lead-Acid Battery	Li-ion Battery
Lifetime (yr)	15	15	8	8

Baseline Design and Sensitivity Analysis

A baseline case was optimized to represent the "business as usual" approach of providing all electrical power from diesel generators with no energy storage, renewables, or plug-in vehicles. The baseline case optimized the size of two diesel generators to minimize the estimated fuel use over one year. Fuel cost was not considered for the baseline cases because the only option for power generation was diesel generators, thus there was no tradeoff with capital cost. That is, the most cost-efficient option is independent of fuel price.

After the baseline case, the full system was optimized with the whole range of components. The fuel prices considered were $5, $10, and $15 per gallon ($1.32, $2.64, and $3.96 per liter), which represents a typical range for the fully-burdened fuel cost for the U.S. Army.

4 RESULTS & DISCUSSION

The first results are to compare the one-year dispatch strategy from HOMER and from the forward-looking optimal dispatch strategy. Next, the optimal design results are shown, with sensitivity analysis performed while varying fuel price.

4.1 Dispatch strategy comparison

The forward-looking optimal dispatch resulted in total yearly fuel use of 36,000 gallons compared to 39,050 gallons using HOMER's dispatch strategy, a 7.8% reduction. The fuel use difference can be explained by the differences in the dispatch strategy of the energy storage. Summary plots were generated showing statistical analysis of the energy storage use over the entire year for both HOMER's dispatch strategy and the forward-looking strategy (Fig. 9). The plots show both the mean battery power for each hour of the day as well as the distribution around the mean.

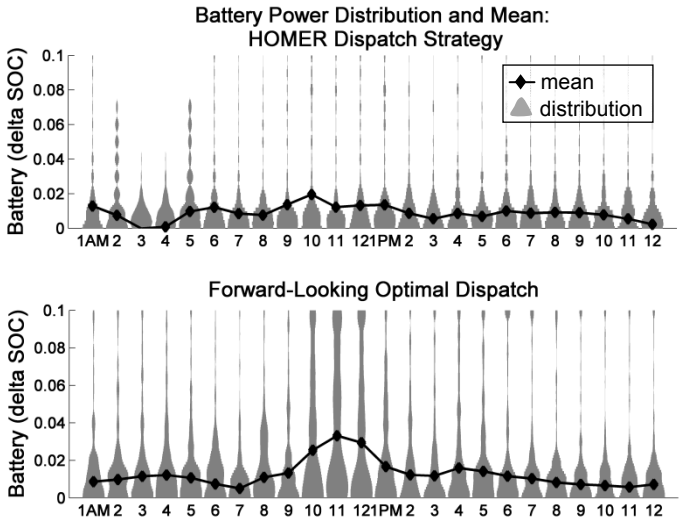

Figure 9. Hourly mean and distribution of battery power: (top) HOMER, (bottom) forward-looking optimal dispatch

The forward-looking optimal dispatch is able to plan the battery storage over multiple time periods, resulting in higher power battery use in the middle of the day (10am – 1pm) compared to HOMER, as shown in Fig. 9. This shows that the optimal dispatch can plan for both the presence and absence of solar energy, whereas HOMER's single-time period dispatch strategy cannot plan ahead for these occurrences.

To see this effect in more detail, an example of the power and energy states of the system are plotted for a single day (June 1st) in Fig. 10. This figure only shows the results from the forward-looking optimal dispatch to show how it plans the battery state-of-charge.

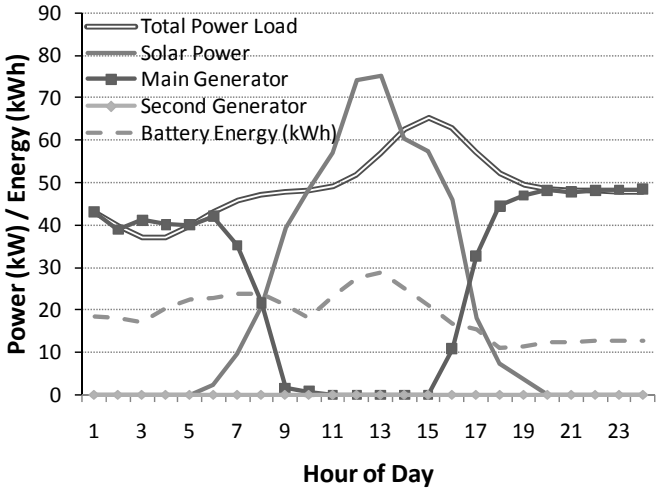

Figure 10. Microgrid power and energy states for June 1st (forward-looking optimal dispatch only)

As seen in Fig. 10, the forward-looking dispatch can predict that the solar supply will exceed the total power load beginning around 11am. Therefore, from hour 7 to 10 the strategy reduces

the generator load and instead uses stored battery energy to supply the load. Then, from hour 10 to 13 the excess solar power is stored in the battery, replenishing its SOC. Finally, as solar power falls below the peaking power demand from hour 14 to 18, energy is again drawn from the battery while the generator is slowly ramped up. These actions help reduce the fuel use of the generator, especially in the transitional periods where load is high but solar supply is low. Note that the battery is not used significantly overnight because its capacity (48 kWh) is only enough to supply the entire load for a single hour. Instead, the strategy decides to operate a single generator at high load to supply the overnight power demands.

The difference in fuel use of the forward-looking strategy is modest relative to HOMER, which shows that HOMER is a useful tool for quickly designing small microgrid systems. However, its use of full-factorial DOE to generate designs limits its scalability to larger systems, and it also has the limitation of not being able to implement coupled systems such as PEVs, nor the ability to combine its dispatch strategy with nested energy management strategies, such as a separate PEV charging strategy. Therefore, the designs generated by HOMER may differ from designs generated with a forward-looking optimal dispatch strategy, especially for energy storage size.

4.2 Optimal microgrid design

The optimization results for the baseline design (generators only) and various fuel prices are shown in Table 7. The total fuel cost for the baseline design is relative to a $5/gallon fuel price, though as previously mentioned the fuel use is independent of fuel price for these cases, so the total fuel cost for any price can easily be calculated.

Table 7. Optimization results compared to baseline case

	Baseline	**Designs with Renewables**		
	$5/gal	**$5/gal**	**$10/gal**	**$15/gal**
Total Cost	$ 272,540	$ 286,040	$ 491,000	$ 678,290
Fuel Cost	$ 268,100	$ 259,500	$ 383,000	$ 539,700
Capital Cost	$ 4,440	$ 26,540	$ 108,000	$ 138,590
Main Gen. (kW)	11.9	60.0	23.0	48.9
Solar Panel (kW)	-	22.6	105.6	136.7
Main Battery (kWh)	-	83.7	86.7	95.6
Secondary Gen.(kW)	110.7	58.9	70.0	62.6
Vehicle Batt. (kWh)	-	9.9	4.7	9.0
Number of Vehicles	-	1	1	1
Fuel Use (gallons)	53,620	51,900	38,300	35,980
% Fuel Reduction	**-**	**3%**	**29%**	**33%**

The results show that the optimal design increases the amount of renewable power and storage battery capacity as fuel price increases, thus reducing fuel use. The optimal design at $5/gallon shows fuel use reduction of 3%; however, the overall cost increases slightly from the two-generator case due to the high expense of the solar panels. As the fuel price increases, the fuel reduction increases up to 33%; the major design changes are that the solar panel power and stationary battery size increase. For these cases, the marginal cost of the additional solar panels is less than the marginal cost of the fuel saved. Thus, fuel use is decreased as well as overall yearly cost as shown in Fig. 11.

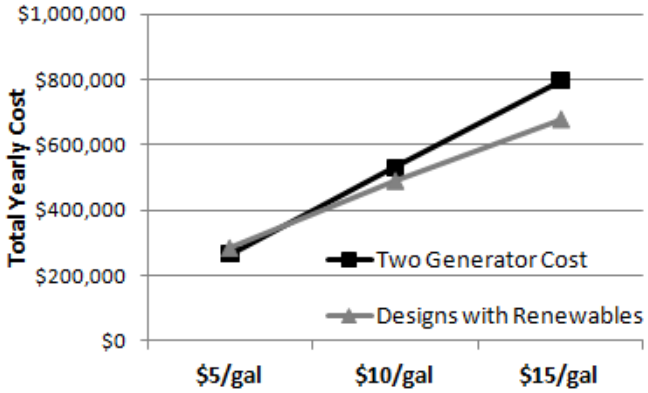

Figure 11. Sensitivity of total yearly cost (operating + capital) to fuel price

The 137 kW solar panel array proposed for the $15/gallon case may be impractical, simply due to its size. However, what this analysis shows is that as the fuel cost increases, the high cost of solar panels is justified, even if the overall size that can be implemented is limited.

The results also show that the optimal system only uses the minimum number of vehicles. In fact, if the optimization were allowed to have zero plug-in vehicles it is expected this option would be chosen. The reason for this is that the benefits of the PEVs, energy storage and generation, are dominated by less expensive, higher efficiency stationary storage and generators. This is especially true because the PEVs generate electricity at low efficiency (22%) relative to the stationary generators because the PEV engines and generators are mismatched in power (200 kW vs. 30 kW), thus the engines operate at low load when running the generators.

The PEVs would be more useful to the microgrid in the absence of stationary batteries and/or stationary generators. However, the generation efficiency would still be low and the fuel use would be relatively high. In this case, the fuel use could be reduced if the vehicles' engines and generators were similar sizes, thus allowing the engines to run at high load and high efficiency.

Though this case study is focused on an islanded military base, the conclusions are applicable to civilian situations where fuel price is relatively high (e.g., the European Union, island communities) and there is no infrastructure to connect to an external electrical grid. For cost-effectiveness and additional fuel use reduction in the civilian case, it would be beneficial to study the use of wind power and combined heat and power in addition to the PV/battery system studied here.

5 CONCLUSIONS

Forward-looking optimal dispatch can be a useful approach for designing microgrids with energy storage elements. The ability to forecast future scenarios enables greater flexibility in use of storage, which can result in designs with lower fuel use. The strategy presented herein is capable of dispatching plug-in

vehicles with variable connectivity to the microgrid and can model coupled components such as an engine that operates passively to charge a vehicle battery under states of low battery SOC. This forward-looking optimal dispatch strategy can be nested in an optimal design formulation, which is more scaleable than full-factorial design approaches and can generate designs with better use of energy storage.

Under the islanded forward-operating base scenario presented here, design optimization results show that the minimum cost designs reduce fuel use from 3–30% by using a microgrid of renewable energy, storage batteries, and plug-in vehicles to augment the typical generator-based electrical supply. This fuel reduction comes from the renewable energy source with a forward-looking electrical storage strategy, downsized generators, and increased generator load, which increases efficiency. The capital cost of this system can be justified when the fuel cost is greater than $5/gallon ($1.32/liter), which is at the low end of the fully-burdened cost of fuel for a U.S. Army forward base. Above this fuel price, the addition of renewables and energy storage can save both fuel and overall cost. This economic analysis does not consider the additional savings due to reduced re-supply trucks necessary to provide fuel to the base. The fuel saved for this base is equivalent to 7 military tanker trucks per year, which saves not only additional fuel but reduces the risk to soldiers to improvised explosive devices (IEDs) and other supply-line dangers. However, practical issues may limit the size of solar panels, storage batteries, etc. that can be added to a small base, due to transport logistics, maintenance, and vulnerability. These are issues for further study.

For this case study, vehicles are not chosen to be a large contributor to the microgrid. This is because their benefits, energy storage and energy generation via the engine, are also present in other more efficient and lower cost options. Thus, the stationary storage batteries and stationary generators are chosen instead of additional vehicles. However, for bases where either the stationary batteries and/or generators are not present, the vehicles would then become useful. In addition, the vehicles could provide immediate, short-term grid support under crisis situations where there is a loss of power generation capacity. These scenarios are planned for future studies.

Though these results are applied to an islanded military base, they are applicable to civilian cases where fuel price is greater than $5/gallon ($1.32/liter) and there is no infrastructure available to connect to an external electrical grid. Examples of this situation include island communities, remote towns, etc.

This study is limited by the assumptions made for model inputs and the specifics of the location and microgrid studied. Improvements should include actual measured power load data and more realistic, nonlinear submodels for the batteries and PV array. In addition, this model was solved deterministically assuming perfect future knowledge. Ideally, this system should be optimized while considering the uncertainties in solar availability, power load, vehicle plug-in, etc. Furthermore, this study only looked at a single microgrid topology with fixed components. Future studies should include variable numbers and types of components, as well as the addition of wind power and other renewable energy sources as options.

Future work should also investigate the use of optimal control techniques. Such techniques may include Model Predictive Control (MPC) and various methods for trajectory optimization. A variety of computationally efficient methods have been developed for the trajectory optimization problem, including pseudospectral methods [24–26]. By formulating the microgrid scheduling problem in state-space form, such methods can be applied to the problem of optimal power dispatch of the microgrid.

ACKNOWLEDGMENTS

This research is supported by the Automotive Research Center, a US Army Center of Excellence in Modeling and Simulation of Ground Vehicles, headquartered at the University of Michigan. This support is gratefully acknowledged. Additional thanks are given to HOMER Energy for making its microgrid design software available.

REFERENCES

[1] Shaffer, E.C., Massie, D.D., and Cross, J.B., 2006, “Power and Energy Architecture for Army Advanced Energy Initiative,” Army Research Laboratory Report, Adelphi, Maryland.

[2] Tselepis, S., 2010, “Greek Experience with Microgrids: Results from the Gaidouromantra Site, Kythnos Island”, *Vancouver 2010 Symposium on Micrgrids*, 22 July, Vancouver, B.C., Canada.

[3] Ashok, S., 2007, “Optimised Model of a Community Hybrid Energy System,” *J. of Renewable Energy*, **32**(7), pp. 1155-1164.

[4] Gupta, A., Saini, R.P., and Sharma, M.P., 2010, “Steady-state Modelling of Hybrid Energy System for Off Grid Electrification of Cluster of Villages,” *J. of Renewable Energy*, **35**(2), pp. 520-535.

[5] del Real, A. J., Galus, M. D., Bordons, C., and Andersson, G., 2009, “Optimal power dispatch of energy networks including external power exchange,” *European Control Conference (ECC)*, 23-26 August, Budapest, Hungary.

[6] Hawkes, A.D., and Leach, M.A., 2009, “Modelling high level system design and unit commitment for a microgrid,” J. *of Applied Energy*, **86** (7-8), pp. 1253–1265.

[7] Stadler, M., Marnay, C., Siddiqui, A., Lai, J., Coffey, B., and Aki, H., 2009, “Effect of Heat and Electricity Storage and Reliability on Microgrid Viability: A Study of Commercial Buildings in California and New York States,” Ernest Orlando Lawrence Berkeley National Laboratory, Report LBNL-1334E-2009.

[8] Asano, H., Bando, S., and Watanabe, H., 2007, “Methodology to Design the Capacity of a Microgrid,” *IEEE International Conference on System of Systems Engineering*, 16-18 April, San Antonio, TX.

[9] Mohamed, F.A., and Koivo, H.N., 2009, "System modeling and optimal management of a Microgrid using Mesh Adaptive Direct Search*," J. of Electrical Power and Energy Systems*, **32**(5), pp. 398-407.

[10] Lambert, T., Gilman, P., Lilienthal, P., 2006, "Chapter 15: Micropower System Modeling with Homer", in *Integration of Alternative Sources of Energy* by Felix A. Farret and M. Godoy Simoes, John Wiley & Sons, Inc.

[11] Lu, S., Schroeder, N.B., Kim, H.M., Shanbhag, U.V., 2010, "Hybrid Power/Energy Generation Through Multidisciplinary and Multilevel Design Optimization with Complementarity Constraints," *ASME Journal of Mechanical Design*, **132**(10), pp. 101007 -101019.

[12] Arnold, M., Negenborn, R.R., Andersson, G., and De Schutter, B., 2009, "Multi-Area Predictive Control for Combined Electricity and Natural Gas Systems," *European Control Conference (ECC)*, 23-26 August, Budapest, Hungary.

[13] Momber, I., Gómez, T., Venkataramanan, G., Stadler, M., Beer, S., Lai, J., Marnay, C., and Battaglia, V., 2010, "Plug-in Electric Vehicle Interactions with a Small Office Building: An Economic Analysis using DER-CAM," *Proceedings of the 2010 IEEE PES General Meeting*, 26-29 July, Minneapolis, MN.

[14] Geidl, M. and Andersson**,** G., 2006, "Operational and Structural Optimization of Multi-Carrier Energy Systems," *European Transactions on Electrical Power*, **16** (5), pp. 463-477.

[15] Geidl, M., 2007, "Integrated Modeling and Optimization of Multi-Carrier Systems," Doctoral dissertation, ETH Zurich.

[16] Fathy, H. K., Reyer, J. A., Papalambros, P. Y., and Ulsoy, A. G., 2001, "On the Coupling Between the Plant and Controller Optimization Problems," *IEEE American Control Conference*, 25-27 June, Arlington, VA.

[17] Jones, D.R., 2001, "DIRECT Global Optimization Algorithm", *Encyclopedia of Optimization*, eds. C. Floudas and P. Pardalos, Kluwer Academic Publishers, pp. 431-440.

[18] Hartranft, T.J., Yeboah, F., Grady, D., and Ducey, R., 2007, "Proceedings of the 1st Army Installation Energy Security and Independence Conference", Construction Engineering Research Laboratory Report ERDC/CERL TR-07-9, U.S. Army Corps of Engineers.

[19] Cummins Power Generation, "Specifications and Data Sheets," http://cumminspower.com/en/technical/documents, accessed January 10, 2011.

[20] Average Monthly Temperatures in Kabul, Afghanistan, http://www.weather.com/outlook/health/allergies/wxclimatology/monthly/graph/AFXX0003, accessed January 6, 2011.

[21] Lawrence Berkeley National Laboratory, "DER technology Data Used after 2004," compiled by Ryan Firestone, http://der.lbl.gov/der-cam/technology-data-archive, accessed December 6, 2010.

[22] Vyas, A.D., Henry K. Ng, Danilo J. Santini, and John L. Anderson, 1997, "Batteries for Electric Drive Vehicles: Evaluation of Future Characteristics and Costs through a Delphi Study," Argonne National Laboratory, *SAE International Spring Fuels and Lubricants Meeting*, May 5-7, Detroit, Michigan.

[23] Peterson, J., 2009, "Li-ion Batteries and How Cheap Beat Cool in the Chevy Volt," *Seeking Alpha*, March 23.

[24] Betts, J.T., and Frank, P.D., 1994, "A Sparse Nonlinear Optimization Algorithm", *J. of Optimization Theory and Applications*, **82**(3), pp. 519-541.

[25] Betts, J.T., 1998, "Survey of Numerical Methods for Trajectory Optimization", *J. of Guidance, Control and Dynamics*, **21**(2), pp. 193-207.

[26] Ross, M., and Fahroo, F., 2003, "Legendre Pseudospectral Approximations of Optimal Control Problems", in *New Trends in Nonlinear Dynamics and Control*, LNCIS 295, Springer-Verlag, Berlin, pp. 327 – 342.

